












RESEARCH PAPER

 OPEN ACCESS 

## A role for GLUT3 in glioblastoma cell invasion that is not recapitulated by GLUT1

Catherine J Libby <sup>a</sup>, Sajina Gc <sup>a</sup>, Gloria A. Benavides<sup>b</sup>, Jennifer L. Fisher<sup>a</sup>, Sarah E. Williford<sup>a</sup>, Sixue Zhang <sup>c</sup>, Anh Nhat Tran <sup>d</sup>, Emily R. Gordon <sup>e</sup>, Amber B. Jones <sup>a</sup>, Kaysaw Tuy <sup>a</sup>, William Flavahan<sup>f</sup>, Juan Gordillo<sup>a</sup>, Ashlee Long<sup>g</sup>, Sara J. Cooper <sup>e</sup>, Brittany N. Lasseigne<sup>a,h,i,j,k</sup>, Corinne E. Augelli-Szafran<sup>c</sup>, Victor Darley-Usmar<sup>b</sup>, and Anita B. Hjelmeland <sup>a,h</sup>

<sup>a</sup>Department of Cell, Developmental and Integrative Biology, University of Alabama at Birmingham, Birmingham, AL, USA; <sup>b</sup>Mitochondria Medicine Laboratory, Department of Pathology, University of Alabama at Birmingham, Birmingham, AL, USA; <sup>c</sup>Chemistry Department, Drug Discovery Division, Southern Research, Birmingham, AL, USA; <sup>d</sup>Department of Neurosurgery, Northwestern University, Chicago, IL, USA; <sup>e</sup>HudsonAlpha Institute for Biotechnology, Huntsville, AL, USA; <sup>f</sup>Department of Molecular, Cell and Cancer Biology, University of Massachusetts Medical School, Worcester, MA, USA; <sup>g</sup>Department of Genetics, University of Alabama at Birmingham, Birmingham, AL, USA; <sup>h</sup>O'Neal Comprehensive Cancer Center, University of Alabama at Birmingham, Birmingham, AL, USA; <sup>i</sup>Hugh Kaul Precision Medicine Institute, University of Alabama at Birmingham, Birmingham, AL, USA; <sup>j</sup>The Center for Clinical and Translational Science, University of Alabama at Birmingham, Birmingham, AL, USA; <sup>k</sup>UAB IMPACT Fund, University of Alabama at Birmingham, Birmingham, AL, USA

### ABSTRACT

The multifaceted roles of metabolism in invasion have been investigated across many cancers. The brain tumor glioblastoma (GBM) is a highly invasive and metabolically plastic tumor with an inevitable recurrence. The neuronal glucose transporter 3 (GLUT3) was previously reported to correlate with poor glioma patient survival and be upregulated in GBM cells to promote therapeutic resistance and survival under restricted glucose conditions. It has been suggested that the increased glucose uptake mediated by GLUT3 elevation promotes survival of circulating tumor cells to facilitate metastasis. Here we suggest a more direct role for GLUT3 in promoting invasion that is not dependent upon changes in cell survival or metabolism. Analysis of glioma datasets demonstrated that GLUT3, but not GLUT1, expression was elevated in invasive disease. In human xenograft derived GBM cells, GLUT3, but not GLUT1, elevation significantly increased invasion in transwell assays, but not growth or migration. Further, there were no changes in glycolytic metabolism that correlated with invasive phenotypes. We identified the GLUT3 C-terminus as mediating invasion: substituting the C-terminus of GLUT1 for that of GLUT3 reduced invasion. RNA-seq analysis indicated changes in extracellular matrix organization in GLUT3 overexpressing cells, including upregulation of osteopontin. Together, our data suggest a role for GLUT3 in increasing tumor cell invasion that is not recapitulated by GLUT1, is separate from its role in metabolism and survival as a glucose transporter, and is likely broadly applicable since GLUT3 expression correlates with metastasis in many solid tumors.

### ARTICLE HISTORY

Received 22 May 2020  
Revised 16 January 2021  
Accepted 19 February 2021

### KEYWORDS



Glucose transporter;  
glioblastoma; invasion;  
metabolism


## Introduction

Altered metabolism is a hallmark of cancer [1] and has been implicated in the regulation of cancer invasion and metastasis [2–6]. One highly invasive and metabolically plastic tumor type is glioblastoma (GBM). Glioblastoma is the most common primary malignant adult brain tumor with a propensity to invade into the surrounding brain [7–10]. The invasive nature of this disease leads to recurrence, which is often within centimeters of the original tumor site, and ultimately death in nearly all patients [5,9,11,12]. The invasive nature of GBM makes it an incredibly difficult tumor to treat: these tumor cells invading normal brain cannot be removed by surgical resection and do not readily

respond to current therapies. Improved understanding of the mechanisms of invasion and metabolism, as well as the links between them, in tumor growth, maintenance, and spread is likely to lead to novel treatments that will ultimately extend patient life expectancy.

The glycolytic shift of tumor cells is known to involve the SLC2A family of glucose transporters (GLUT) [13–13–16]. In the brain, glucose transporter 3 (GLUT3) is recognized as the neuronal glucose transporter, and glucose transporter 1 (GLUT1), is important for glucose uptake in astrocytes and the transport of glucose across the blood brain barrier [14,17–19]. GLUT1 is also ubiquitously expressed throughout the body. Differences in tissue expression between GLUT3 and GLUT1 may

**CONTACT** Anita B. Hjelmeland  [hjelmea@uab.edu](mailto:hjelmea@uab.edu)  Assistant Professor Department of Cell, Developmental and Integrative Biology University of Alabama at Birmingham Birmingham, AL 35294

 Supplemental data for this article can be accessed [here](#).

© 2021 The Author(s). Published by Informa UK Limited, trading as Taylor & Francis Group.

This is an Open Access article distributed under the terms of the Creative Commons Attribution License (<http://creativecommons.org/licenses/by/4.0/>), which permits unrestricted use, distribution, and reproduction in any medium, provided the original work is properly cited.

correlate with differential requirements for energy: GLUT3 has a five-fold higher affinity for glucose compared to GLUT1, allowing for preferential glucose uptake in environments with lower glucose concentrations [14,20]. Indeed, elevation of GLUT3 in subsets of less differentiated, highly metabolically plastic GBM cells called brain tumor initiating cells (BTICs) promotes survival in restricted glucose [2,21]. BTICs have also previously been reported to be more invasive than more differentiated cells within GBM tumors [22,23]. GLUT3 expression was also elevated in bevacizumab-resistant cells [24], and bevacizumab resistance is associated with a shift in metabolism, as well as a more invasive and mesenchymal-like phenotype [5,25–28]. However, a direct role for GLUT3 in modulating GBM invasion has not yet been reported.

Epithelial to mesenchymal transition and metastatic disease has been correlated with GLUT3 expression in other solid tumors such as those of the breast [29,30], liver [31], and lung [32]. Recently published papers demonstrated that GLUT3 was elevated in circulating tumor cells that have a propensity to target the brain [29] and that GLUT3 was necessary for their survival within the brain [30]. Further reports have linked GLUT3-YAP signaling to colon cancer metastasis [33], a pathway that is of conserved importance in some subsets of GBM cells [34]. Importantly, the data suggest that glycolytic shift/elevated glucose uptake mediated by GLUT3 increase circulating tumor cell survival which in turn promotes metastasis. High GLUT3 expression positively correlated with an increased incidence of metastasis in breast and head and neck cancers [35]. Furthermore, lower levels of GLUT3 correlated with a longer duration of metastasis-free survival in breast and head and neck cancers [36]. Through the use of publicly available data sets, we also observed a significant increase in GLUT3 expression in metastatic ovarian, head and neck, and colon cancers compared to primary tumors (Supplementary Figure 1) [37,38]. While these data suggest a role for GLUT3 in invasion and metastasis, a direct role for GLUT3 in invasion independent of pro-survival effects has yet to be investigated. Through our study, we have determined that GLUT3 has a role in mediating glioma invasion, outside of its role in metabolism, that is mediated by the C-terminal end of the protein.

## Results

### *GLUT3 is elevated in invasive GBM cells*

We previously reported that GLUT3 expression is correlated with worse glioma prognosis and is elevated in

BTICs allowing them to preferentially survive in the low nutrient microenvironments commonly present in GBM tumors [21]. In order to further understand the relevance of elevated GLUT3 in GBM biology, we analyzed the Ivy Glioblastoma Atlas Project database and found GLUT3 (SLC2A3), but not GLUT1 (SLC2A1), expression was significantly elevated at the leading edge of GBMs (Figure 1 a,b) [35]. A correlation between elevated GLUT3, but not GLUT1, expression and white matter tract invasion was also noted in VASARI REMBRANDT data (Figure 1 c,d) [36,39]. This opens the possibility that invasion mediated by GLUT3 could contribute to the poorer patient prognosis associated with elevated GLUT3 expression.

### *Elevated GLUT3 expression promotes GBM invasion in vitro*

To identify whether GLUT3 has a distinct role in cellular invasion, we overexpressed GLUT1-V5 or GLUT3-V5 cDNA using lentiviral infection in D456 and JX22 GBM patient derived xenograft (PDX) and U251 GBM cells. Expression of GLUT1-V5 or GLUT3-V5 was confirmed via qRT-PCR or western blot analysis after selection with Blasticidin S (Figure 1e, Supplementary Figure 2a). Overexpression levels of GLUT1 and GLUT3 were kept comparable to one another to limit potential dosing artifacts due to the overexpression system. To assess invasive capacity of GLUT3 or GLUT1 overexpressing cells, we utilized Boyden chamber assays with both glucose and growth-factors as chemo-attractants in the bottom well (Figure 1 f-i, Figure 2a-d,b-e). GLUT3 overexpressing cells, but not GLUT1 overexpressing cells, had significantly increased invasion compared to vector control cells in the Boyden chamber-based cell invasion assay (Figure 1 f-i, Figure 2a-d, Supplemental Figure 2b-e). In D456 cells overexpressing GLUT3, invasive cell counts were elevated by at least 50% of controls (Figure 1i). Interestingly, we observed no significant differences in D456 cells in the Boyden chamber-based cell migration assay (Figure 1 j). However, we did see an elevation in growth in GLUT1 overexpressing D456 cells indicating the potential for a ‘go versus grow’ phenomenon occurring in these cells (Figure 1k). These experiments were repeated in U251 cells where we obtained similar results in the invasion and migration assays. In U251 cells, GLUT3 overexpression increased invasion by 75% (Supplemental Figure 2b-e), but again we saw no differences in migration experiments (Supplemental Figure 2 f). In U251 cells, there were no differences in growth after 36 hours between the control, GLUT1

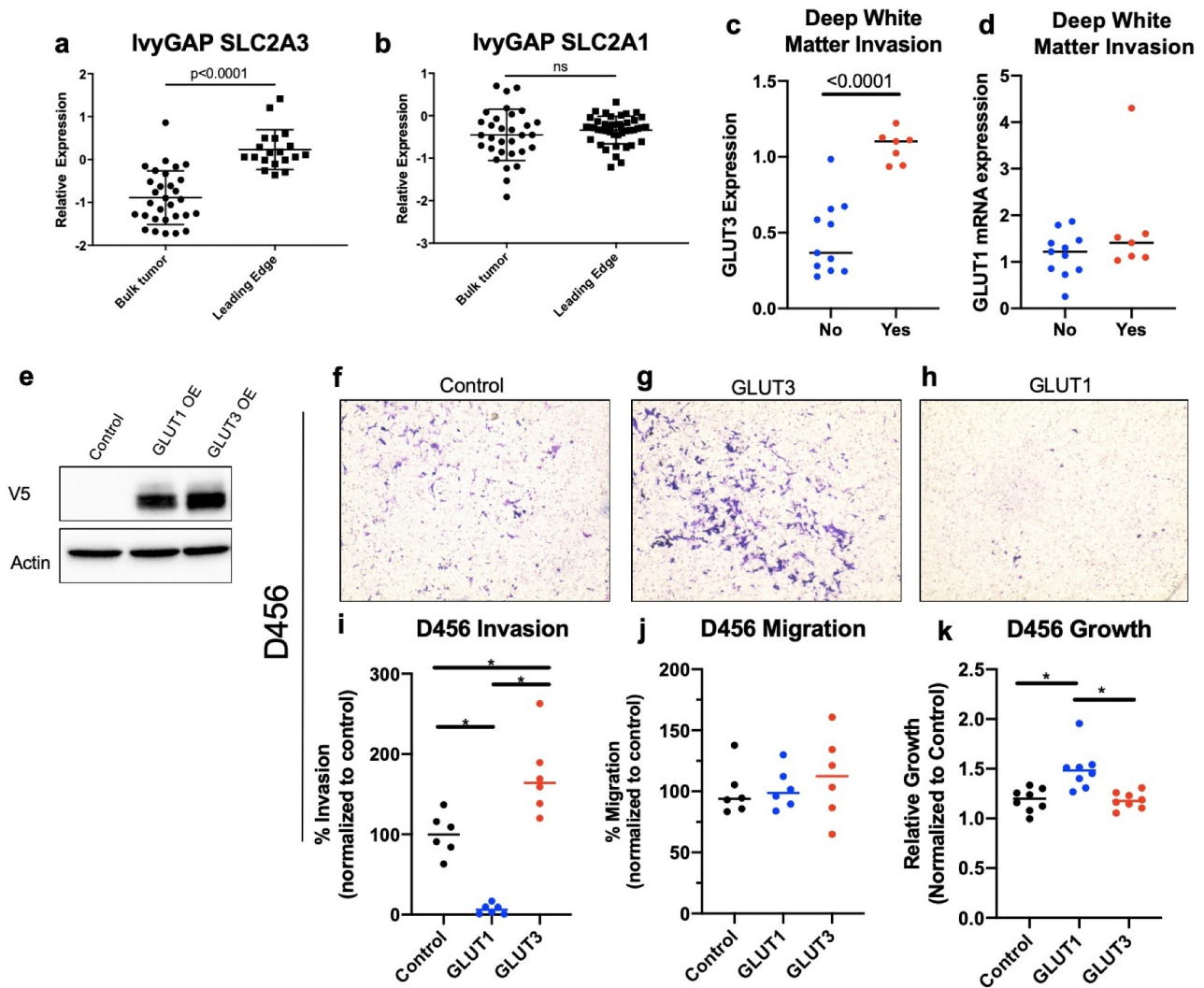


**Figure 1.** Increased GLUT3 expression correlates with increased GBM invasion in 0456 GBM cells.

Analysis of IvyGap (a,b) and Rembrandt (c,d) data indicates that GLUT3 (a,c), but not GLUT1 (b,d) mRNA is significantly elevated at the GBM leading invasive edge. (e) Western blot of 0456 GBM expressing control, GLUT1-V5 cDNA, or GLUT3-V5 cDNA lentivirus plasmids with analysis for V5 and actin levels. (f-k) 0456 GBM cells were incubated under low glucose conditions 16 hours prior to plating in invasion or migration Boyden chamber assays under low glucose and growth factor starvation with chemotaxis toward high glucose and growth factors. Representative images of invasion inserts at 10x magnification for 0456 (f-h) that were quantified using ImageJ (i). Migration was assessed using non-coated inserts and quantified using ImageJ (k) Analysis of 0456 growth under low glucose conditions for 36 hours, a time course similar to the total time of invasion assays. Data are average of the sum of six images per insert from three experiment for invasion and migration ( $n = 2$ ). Growth results are from three experiment  $n = 3$ ,  $\pm$  sd, one-way ANOVA and Tukey's multiple comparison test ( $\ast$ ,  $p < 0.05$ ).

overexpressing, and GLUT3 overexpressing cells (Supplemental Figure 2 g).

As U251 cells are a standard GBM cell line and the D456 PDX has a proneural subtype gene signature, we also utilized PDX cells of a mesenchymal subtype, JX22, for further investigation of the role of GLUT3 in invasion. Invasion was elevated by approximately 200% in JX22 cells overexpressing GLUT3 (Figure 2a-d) and no differences in growth were observed (Figure

2e). The lack of significant growth elevation in GLUT3 overexpressing cells indicates the observed invasion phenotype is not due to a proliferation advantage in these cells. In order to assess GLUT3 mediated invasion at physiologically relevant levels of expression that would be seen in tumors, we sorted for the GLUT3<sup>high</sup> population from JX22 GBM PDX cells and observed GLUT3<sup>high</sup> cells also trended to be more invasive than GLUT3<sup>low</sup> cells (Figure 2 f-j).

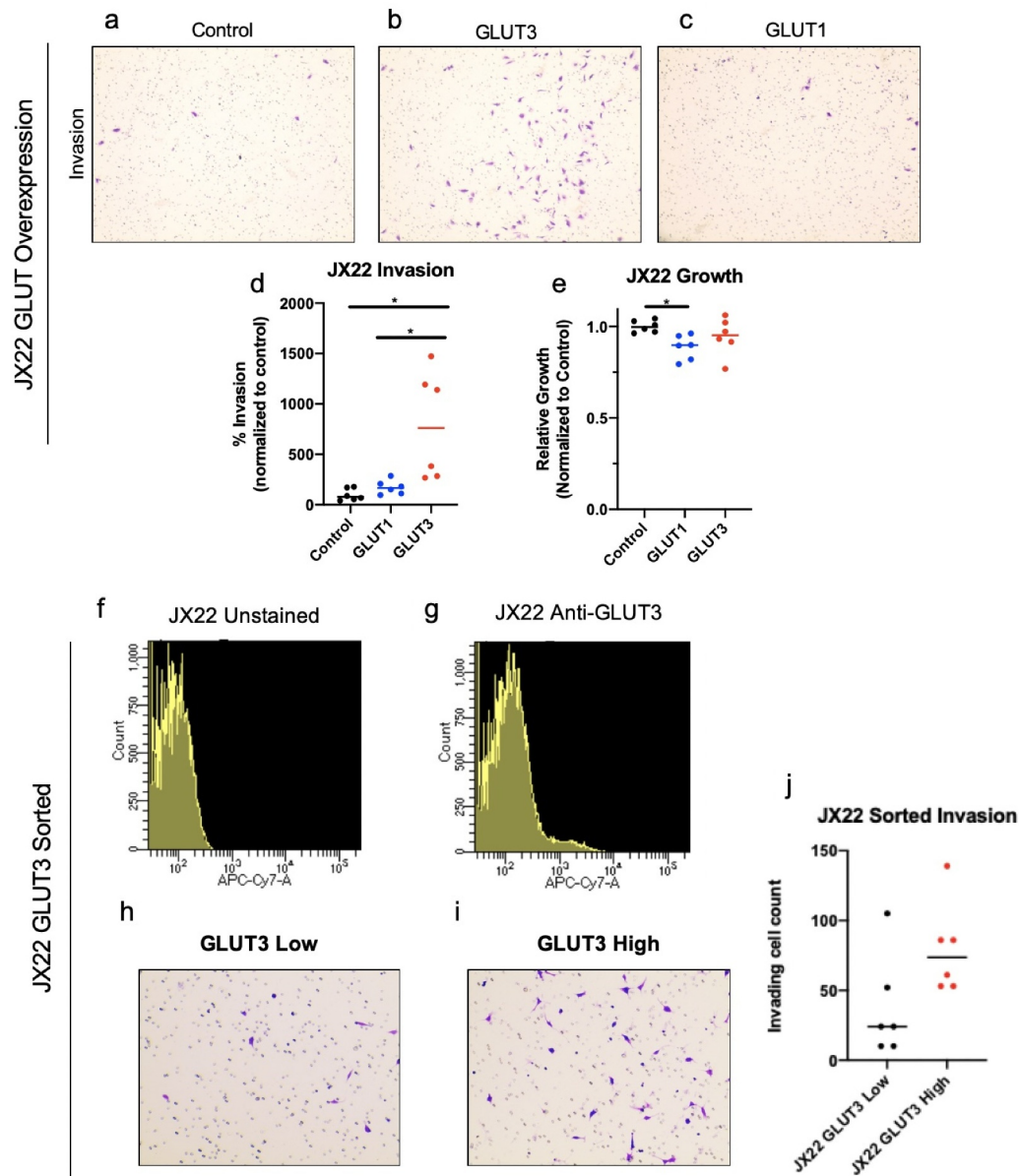


**Figure 2.** JX22 cells with elevated GLUT3 expression display increased invasion. (a-f) Representative images of JX22 GBM cell invasion inserts at 10x magnification exogenous GLUT overexpression (a-c) that were quantified using ImageJ (d). (e) Analysis of 0456 growth under low glucose conditions for 36 hours indicate no significant differences over a time course similar to the invasion assay. Histograms of fluorescent signal for unstained (f) or anti-GLUT3-Alexa Fluor 647 (g) JX22 cells from fluorescence-activated cell sorting. Representative images of invasion inserts for low (h) and high (i) GLUT3 expressing JX22 cells that were quantified using ImageJ. Data are average of the sum of six images per insert from two experiments for invasion ( $n = 3$ ) and for growth results are from two experiments ( $n = 3$ ),  $\pm$  sd, one-way ANOVA and Tukey's multiple comparison test (\*,  $p < 0.05$ ).

### **The intracellular C-terminal tail of GLUT3 is necessary to induce GLUT3-mediated invasion**

The GLUT isoforms are highly homologous proteins, with GLUT1 and GLUT3 having nearly 80% sequence similarity. Comparison of GLUT1 and GLUT3 protein sequences identified two regions of non-homology near one another; one extracellular (EC) and one intracellular (the C-terminal end [CT]) (Figure 3a-c). The extracellular region is

predicted to facilitate glucose recognition and binding and the intracellular region likely to facilitate protein-protein interactions. To determine if these regions may play a role in the invasive phenotype we observed, we generated chimeric proteins by swapping the GLUT1 sequence into the respective site in GLUT3 as to avoid mutations that are unstable and/or misfolded (Figure 3d). Previously, Inukai et al. utilized a similar strategy to assess apical

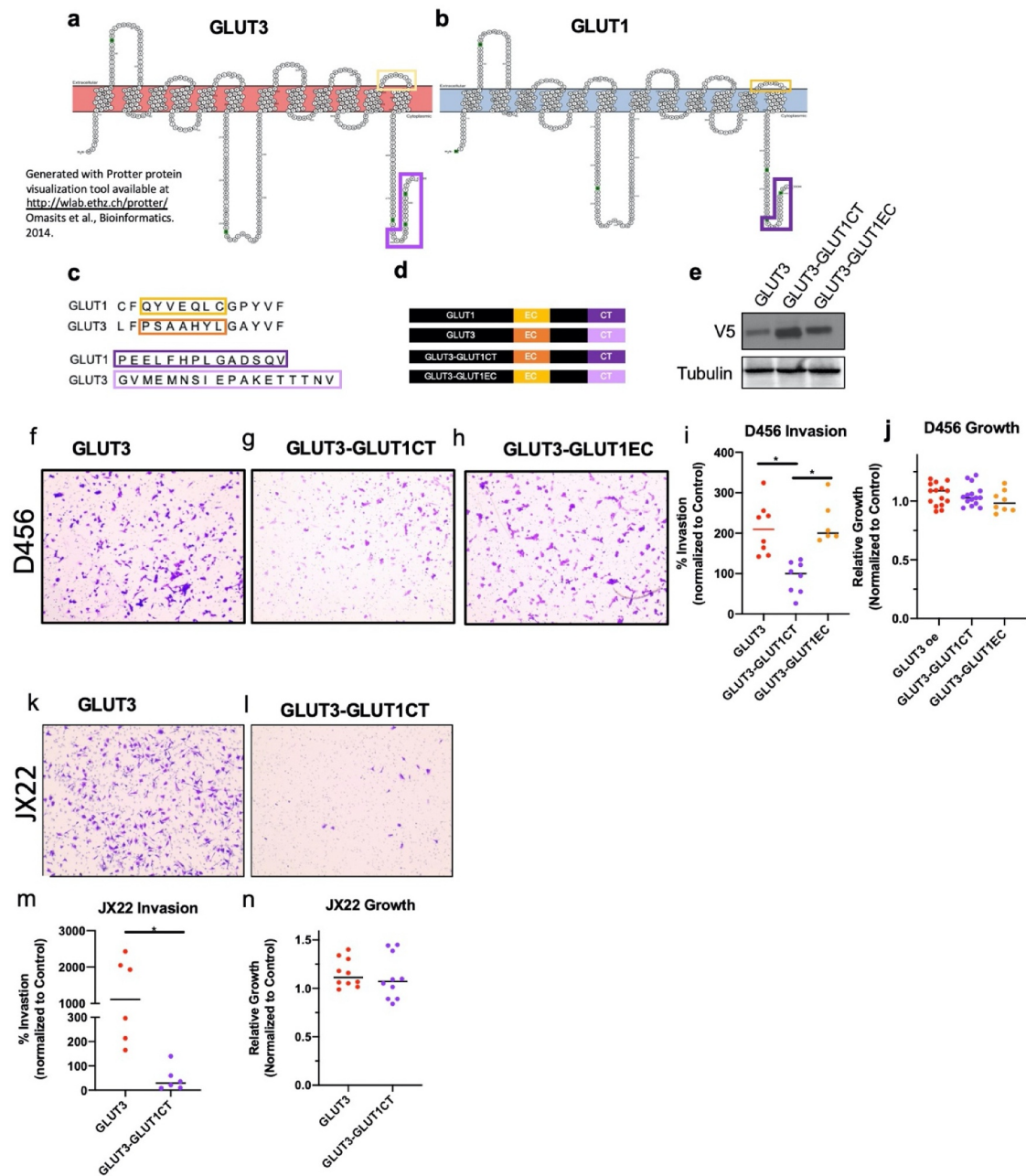


**Figure 3. The intracellular C-terminus, but not extracellular loop 6 is critical for GLUT3 mediated invasion.** Protein scheme of GLUT3 (a) and GLUT1 (b) highlighting regions of non-homology. (c) Sequence alignment of GLUT1 and GLUT3 protein sequences indicating regions of non-homology. (d) Schematic of GLUT3, GLUT1, and GLUT3 chimera proteins generated with immunoblotting in (e) demonstrating expression. (f-h) Representative images of invasion chamber assays at 10x magnification with 0456 cells expressing indicated WT or chimeric proteins that were quantified using ImageJ (i). Analysis of 0456 growth under low glucose conditions for 36 hours indicate no significant differences over a time course similar to the invasion assay. (k, l) Representative images of JX22 cells expressing GLUT3 WT or GLUT3-GLUT1CT chimeric proteins Invasion assay inserts at 10x magnification which are quantified in (m). (n) Representative growth analysis of JX22 GLUT3 WT versus GLUT3-GLUT1CT chimeric protein expressing cells. Data are average of the sum of six images per insert from at least two experiments for invasion ( $n = 2-3$ ) and for growth results are from three experiments ( $n = 3$  or  $4$ ),  $\pm$  sd, one-way ANOVA and Tukey's multiple comparison test (\*,  $p < 0.05$ ).

versus basal membrane localization of GLUT1 and GLUT3 indicating that these chimeras should traffic to the membrane and be functional [40]. Following confirmation of successful expression of wildtype and

chimeric proteins (Figure 3e), we assessed their invasive capacity. GLUT3-GLUT1EC had no effect on GLUT3 mediated glioma cell invasion, with cell quantification levels comparable to that of GLUT3

wildtype in D456 cells (Figure 3 f,h,i). However, GLUT3-GLUT1CT attenuated glioma cell invasion, reducing invasion by over 60% compared to wildtype GLUT3 (Figure 3 f,g,i). Additionally, these chimeric proteins did not alter growth in D456 cells (Figure 3 j). These results were recapitulated with JX22 (Figure 3k-n) and U251 cells (Supplementary Figure 2 h-k), suggesting the potential for this finding to be broadly applicable as these cells span two subtypes of GBM. We then performed the reciprocal experiments, utilizing a GLUT1-GLUT3CT chimeric protein (Figure 4a,b). Substitution of the GLUT1 C-terminus for that of GLUT3 elevated invasion in Boyden chamber assays compared to GLUT1 WT

expressing cells, but again did not significantly alter cell growth (Figure 4 c-j). These data indicate that the C-terminal region of GLUT3 is responsible for mediating the pro-invasive phenotype observed here (Figures 3 and 4). Metabolic flux assays indicated no consistent metabolic changes that were associated with the invasive phenotype (Supplemental Figure 3). GLUT overexpression did not lead to significant changes in the rate of glycolysis indicating that glucose uptake is not a limiting factor for the cell's glycolytic capacity. The minimal shifts in glycolytic metabolism indicate that the invasive phenotype is independent of glycolytic metabolism.

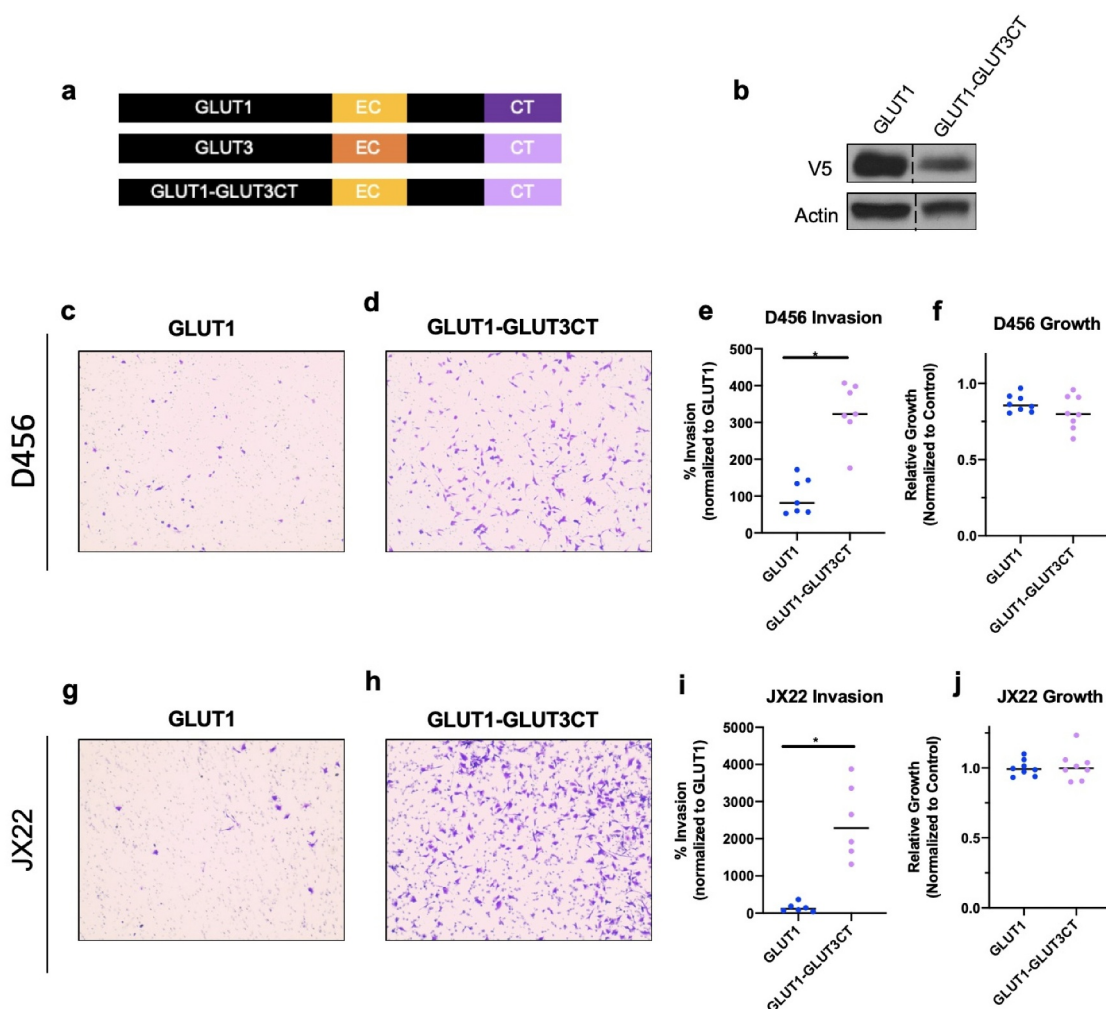


**Figure 4.** The intracellular C-terminus is sufficient to induce invasion in GLUT1 expressing cells. (a) Schematic of GLUT1 and GLUT1-GLUT3CT chimeric proteins generated with immunoblotting in (b) demonstrating expression. (c,d) Representative images of invasion chamber assays at 10x magnification with D456 cells expressing indicated WT or chimeric proteins that were quantified using ImageJ (e). (f) Determination of D456 growth under low glucose conditions for 36 hours (k,j). Representative images of JX22 cells expressing GLUT1 WT or GLUT1-GLUT3CT chimeric protein invasion assay inserts at 10x magnification which are quantified in (m). (n) 36 hour growth analysis of JX22 GLUT1 WT versus GLUT1-GLUT3CT chimeric protein expressing cells. Data are average of the sum of six images per Insert from three experiments ( $n = 2$  or  $3$ ) for Invasion and for growth results are from two experiments ( $n = 4$ ).  $\pm$  sd, one-way ANOVA and Tukey's multiple comparison test (\*,  $p < 0.05$ ).

### Extracellular matrix organization gene signature is altered in GLUT3 overexpressing D456 GBM cells

To begin understanding the molecular differences between GLUT3 and GLUT1 effects that could contribute to invasion, we performed RNA-seq analysis on control, GLUT1 overexpressing and GLUT3 overexpressing D456 GBM cells. We used PathFindR tool to identify gene ontology (GO) terms enriched among genes dysregulated in GLUT3 compared to GLUT1

overexpressing cells. The top three enriched GO terms in GLUT3 compared to GLUT1 overexpressing cells are low-density lipoprotein particle receptor binding, extracellular matrix organization, and retrograde protein transport (endoplasmic reticulum to cytosol) (Figure 5a, Supplemental Figure 4). From this analysis, we noted that multiple elevated transcripts within the extracellular matrix organization GO term, particularly, CD44, osteopontin (SPP1), SPARC, and integrin A3

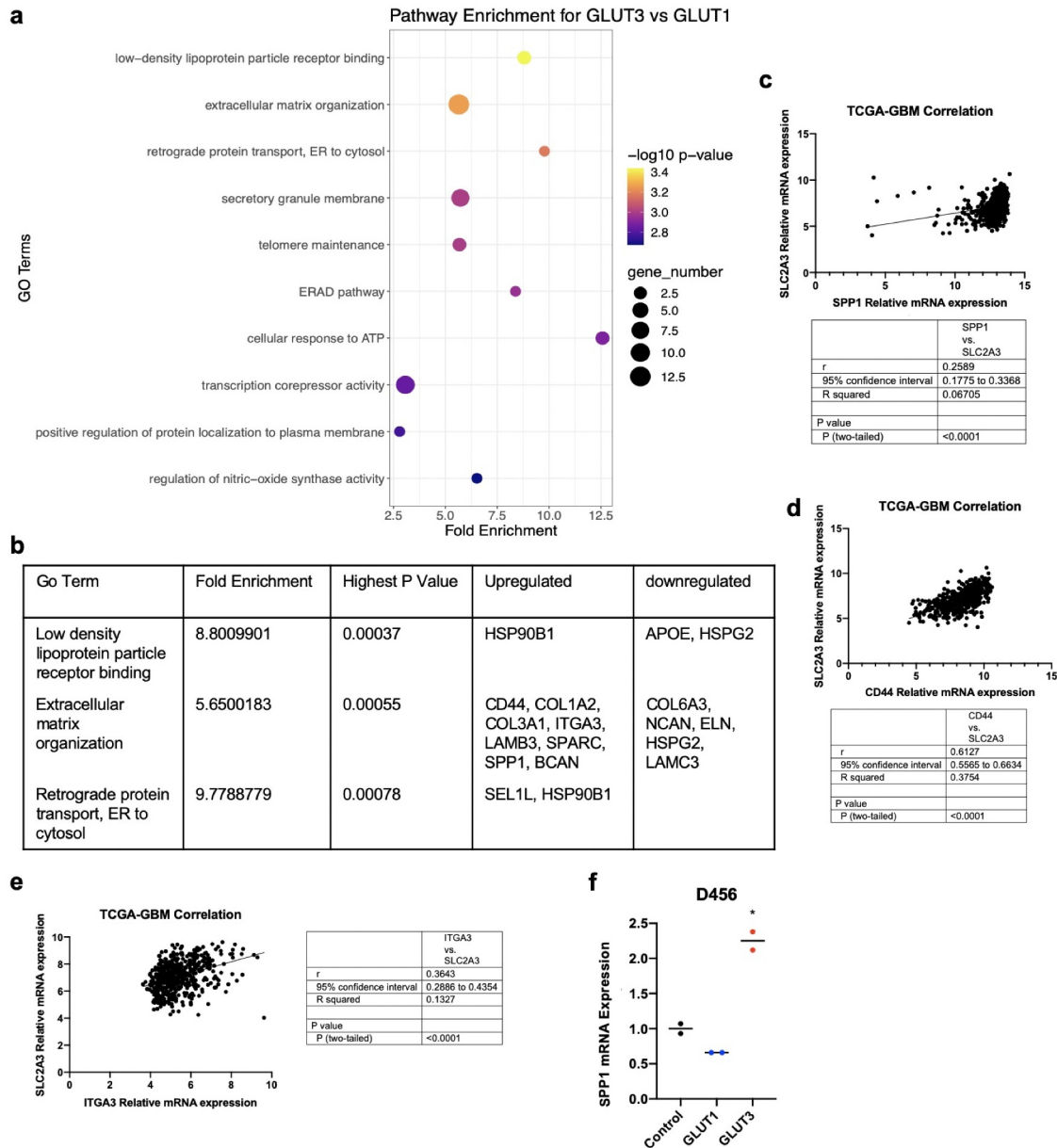


**Figure 5.** Transcriptomic analysis indicates differential regulation of extracellular matrix organization. (a) Dot plot of RNAseq data using the PathfindR package for pathway analysis to identify gene ontology pathway enrichment. (b) Top two enriched GO Terms with their enrichment scores. *p*-values, and differentially regulated genes. Co-expression of SPP1 (c), CD44 (d), and ITGA3 (e) mRNA with SLC2A3 mRNA in the TCGA-GBM dataset. Statistical analysis performed using Pearson's correlation. (d) qRT-PCR of SPP1 in control, GLUT1 overexpressing and GLUT3 overexpressing 0456 cells ( $n = 2$ ), one-way ANOVA and Tukey's multiple comparison test (\*,  $p < 0.05$ ).

(ITGA3) (Figure 5b), have been widely studied in GBM [41–48] and implicated with cancer invasion/metastasis and severity [41–48]. Evaluating the correlation between these genes using The Cancer Genome Atlas (TCGA), we determined that there is a positive correlation between SLC2A3 (GLUT3) and SPP1 (OPN) (Figure 5c), in addition to CD44 (Figure 5d), and ITGA3 (Figure 5e). The upregulation of SPP1 was validated via qRT-PCR, in which there is an over two-fold upregulation of SPP1 mRNA expression in GLUT3 overexpressing D456 cells (Figure 5f). However, we did not see consistent upregulation of several other genes noted in the extracellular matrix organization GO term from the RNA-seq analysis (data not shown).

## Discussion

Previous work has indicated a correlation between GLUT3 and cancer metastasis [29–33] that is thought to depend on the ability of GLUT3 to promote circulating tumor cell survival. However, our results indicate a direct and distinct functional role for GLUT3 in mediating cancer cell invasion that has of yet not been reported to our knowledge. This invasion phenotype was independent of changes to growth or migration, highlighting that this is not a survival advantage due to GLUT3 overexpression. Interestingly, in the D456 cells GLUT1 significantly reduced invasion while also increasing cell growth (Figure 1h,i,k). This could indicate a ‘go versus grow’ phenotype in these cells; however, this was not a broad phenomenon. There may be a subpopulation of cells with a reliance on GLUT1 for sustained proliferation. Alternatively, in U251 cells GLUT1 overexpression resulted in a slight decrease in invasion and growth (Supplemental Figure 2d,e,g) and in JX22 cells there was a nonsignificant minor elevation in invasion, but a decrease in cell growth (Figure 2c,d,e). It is possible that GLUT1 interacts with different protein than GLUT3 and that this influences cellular signaling in ways not yet fully understood. GLUT1 may interact with other proteins to actively inhibit invasion and promote other cellular processes. The lack of invasion associated with high GLUT1 expression may also account for the lack of survival differences between GLUT1 high and low expressing tumors. Very little is known regarding differential functions between the GLUT family members beyond sugar transport and this is an interesting area for future studies.

We show that the pro-invasive phenotype in GLUT3 overexpressing cells is due to its C-terminus (Figures 3 and 4). Chimeric GLUT3 in which the C-terminus was substituted with that of GLUT1 abrogated invasion

(Figure 3). In converse experiments, transferring the GLUT3 C-terminal sequence into GLUT1 increased invasion (Figure 4). The overexpression of GLUT1 or GLUT3 wild type or chimeric proteins had minimal effects on glycolytic metabolic flux that did not correlate with invasive phenotype, thus indicating that the invasive phenotype is independent of glycolytic metabolism. Further studies would be required to identify alternative metabolic pathways that may be activated with GLUT3 elevation, such as changes in lipid metabolism as suggested by the RNAseq data (Figure 5). However, we believe that these differential functions may contribute to the need for multiple isoforms of GLUTs in the body, each expressed in particular tissues [13–16,49,50]. This is also highlighted by the presence of a specific GLUT1 C-terminal binding protein (GLUT1CBP) that binds a PDZ domain within the C-terminus of GLUT1 which facilitates interactions with the cytoskeleton [50]. The region with which the GLUT1CBP is known to interact is not identical to the regions we replaced in our chimera proteins, indicating the potential for multiple regulatory regions within the intracellular C-terminal tail of the GLUT proteins. The report of specific interactions with the GLUT1CT indicates that this may also be true for GLUT3; however, we know of only one study to date specifically assessing differential functions of this region in GLUT3 [40]. The study by Inukai *et al.* generated GLUT1/GLUT3 chimeric proteins where 13 to 290 amino acids from the C-terminus of GLUT3 were transferred into GLUT1 [40]. The chimeric protein containing at least the final 19 amino acids of the GLUT3 c-terminus showed increased localization of GLUT1/GLUT3 chimeric protein to the apical membrane rather than the basal membrane in canine kidney epithelial cells [40]. These data suggest that there can be a specific subcellular localization for GLUT3 that contributes to its function within the cell. Interestingly, the GLUT3 C-terminus shares some homology with regions of proteins that are reported in the literature to play a role in invasion such as TNC, CD40, SPIRE1, GPR98, and PNN [51–57]. These similarities are not shared by GLUT1 indicating that there may be novel protein interactions with GLUT3 that promote invasion. Indeed, it has been reported that GLUT3 is important for trophoblast invasion for successful implantation of embryos during development [58]. Additionally, many metabolic enzymes have been reported to have functions independent of a direct role in metabolism [59–61]. For example, PKM2 is able to phosphorylate histone H3 and SREBPs in addition to its function in glycolysis [59]. Our results widen this to other proteins involved in metabolism, as GLUT3 currently has no known



direct function beyond hexose transport. We believe this is an area that is of great interest and that our studies could lead to a number of intriguing findings for the differential roles of the 14 GLUT family members.

The RNA-sequencing data provide several potential avenues for further investigation to understand the impact of GLUT3 on the extracellular matrix. SPP1, one of the genes upregulated in GLUT3 overexpressing cells (Figure 5), encodes the protein osteopontin (OPN), which has been widely studied in cancers, including glioma. OPN has been shown to mediate cell adhesion and to promote cancer invasion and metastasis [41,62,63]. OPN also interacts with CD44, another molecule shown to be upregulated in the GLUT3 overexpressing cells (Figure 5) [41,62,64]. CD44 is a hyaluronan receptor that has been implicated in regulating cell motility and adhesion to promote cancer metastasis [41,64]. Interestingly, CD44 is commonly associated with a more mesenchymal cell population posing the possibility that high GLUT3 expression induces a mesenchymal shift [65–68]. CD44 and OPN have also been linked to multiple other commonly dysregulated pathways in cancer including but not limited to WNT/beta-catenin and AKT which have also been shown to influence invasion [41,65,69]. While these data suggest that the regulation of OPN and CD44 expression by GLUT3 upregulation deserves to be studied in more depth, we recognize the limitation of these *in vitro* results. The normal brain and brain tumor extracellular matrix and cell–cell interactions are complex and the brain environment will impact cellular behaviors *in vivo*. Evaluation of the GLUT3 invasion phenotype in the context of brain extracellular matrix components including hyaluronan is critical as is evaluation in tumor–endothelial cell interactions considering GBM cells can move along existing blood vessels to invade normal brain [70]. Further analysis of the properties of such as morphology of cancer cells with GLUT3 elevation, including those of other tumor types, with different matrix substrates [71] is an important area of future investigation.

GLUT3 and GLUT1 are the most commonly elevated GLUTs in cancers, including GBM. Their high degree of homology made it incredibly interesting that GLUT3 has such a significant correlation with patient prognosis (both in terms of overall survival and metastatic free survival) that was often not mimicked by GLUT1. The fact that this neuronal glucose transporter is elevated in multiple cancers combined with the distinct invasive role described here in GBM suggests a broader role for GLUT3 in invasion and metastasis.

GBM infiltration into the normal brain ultimately leads to tumor recurrence very near the tumor resection border and this recurrence leads to death in nearly all cases of the disease [5,7–12]. Due to the nature of the brain, excess tissue cannot be resected to expand tumor margins to remove more of the invasive cells. Therefore, drugs that are brain penetrant are highly attractive to improve patient survival. Understanding drivers of GBM invasion will be critical for furthering drug development to improve patient outcomes. Drugs to target GLUT3 could be better designed to inhibit molecular functions outside its role in metabolism as a means to limit potential brain toxicities, potentially by targeting the C-terminal tail or the protein interactions driving GLUT3 mediated invasion. Additionally, GLUT3 targeted therapies would be attractive for a number of other cancers that have an elevation of GLUT3 such as lung, liver, colon, head and neck, and breast cancers where high-grade survival remains poor.

## Methods

**Cells and GBM patient-derived xenografts:** GBM patient derived xenografts D456 and JX22 were obtained from Dr. Darrel Bigner at Duke University and Dr. Jann Sarkaria at Mayo Clinic. The xenografts used here have been assessed for mutation status and relative transcript levels to determine molecular subtypes. Xenografts were dissociated using papain (Worthington Biochemical Corporation) and propagated *in vitro* using DMEM/F12 basal media (Invitrogen) supplemented with epidermal growth factor (EGF), fibroblast growth factor, sodium pyruvate, penicillin/streptomycin, and the B27 equivalent GEM21 (Gemini Bio Products). U251 cells were obtained as a kind gift from Dr. Corinne Griguer. CSC293T cells were generated and propagated as previously described [72]. Low glucose media utilized in some experiments consists of a dilution of 1 mL of NeurobasalA (Gibco) in 9 mL of Neurobasal minus glucose (Gibco), without the addition of any supplements. Prior to plating for experiments, cells were split with Accutase (Gibco) and counted.

**Protter protein visualization for GLUT1 and GLUT3:** Using the Protter [73] online interphase GLUT1 and GLUT3 topology visualizations were generated using the UniProt accession codes GTR1\_Human and GTR3\_Human, respectively. Minor stylistic changes were made to the standard generated image using the tools provided.

**Protein alignment:** Alignment of GLUT1 and GLUT3 sequences was performed using NCBI BlastP

and the FASTA sequences for the Uniprot accession codes above.

**Gene overexpression:** CSC293T cells were transiently co-transfected with psPAX2, pCMV-VSVG and pLX304 lentiviral plasmids containing GLUT3 or GLUT1 (Genecopia) using FuGENE<sup>®</sup> HD Transfection Reagent (Promega) as previously reported [72,74,75]. Virus titer was determined using Lenti-X qRT-PCR Titration Kit (Takara). Addition of Blasticidin S to cell culture media was used to select cells with stable overexpression. pLX304 lentiviral plasmids were mutated to generate chimeric proteins by Bioinnovatis, Inc (Rockville, MD) and plasmids sequenced to verify the desired mutations were present.

**mRNA extraction, cDNA generation and qRT-PCR:** Total mRNA from cells after 16-hour incubation in low glucose media was harvested using TriZol (ThermoFisher) and synthesized into cDNA using the iScript<sup>™</sup> cDNA Synthesis Kit (BioRad). qRT-PCR was performed on the generated cDNA with the SsoAdvanced<sup>™</sup> Universal SYBR<sup>®</sup> Green Supermix (BioRad). The relative expression of GLUT1 and GLUT3 was measured using primer pairs that recognize GLUT1 or GLUT3 cDNA (GLUT1: ACAACCA-GACATGGGTCCAC and GTTAACGAAAAGGCCCA-CAG) (GLUT3: AGCTCTCTGGGATC-AATGCTGTGT and ATGGTGGCATAGATGGGCTCTTGA). Primers against SPP1 were presynthesized from BioRad for PrimePCR applications (qHsaCID0012060). The data were analyzed and normalized against ACTB (AGAAAATCTGGCACCACACC and AGAGGCGT-ACAGGATAGCA) expression to determine relative expression of target genes similar to prior reports [21,76].

**Western blotting and antibodies:** Cells were harvested following 16-hour incubation in low glucose media and lysed using M-PER (Thermo Scientific). Protein concentration was determined using the BCA assay (Thermo Scientific). Prior to electrophoresis on 4–20% Tris-Glycine Mini Gels (Invitrogen), protein lysates were denatured with Novex Tris-Glycine SDS sample buffer and NuPAGE sample reducing agent (Invitrogen). Protein was then transferred to nitrocellulose membranes (BioRad) and blocked using Pierce Protein Free Blocking Buffer. Primary antibodies for Western blot: mouse anti-V5 (Invitrogen) and Rabbit anti-Actin (Sigma). (n = 3)

**Measurement of cell growth:** Cell numbers were determined using crystal violet staining and solubilization in 10% acetic acid [77].  $1 \times 10^4$  cells were seeded in 96-well plates coated with Geltrex (ThermoFisher) to promote cell adhesion and allowed to recover and attach overnight. The following day, the media was

changed to low glucose media and incubated for 36 hours. At the end of experiments, cells were fixed in 10% formalin overnight at 4°C, stained with 0.2% crystal violet, and then washed x3 with diH<sub>2</sub>O to remove excess staining solution. Crystal violet was solubilized using 10% acetic acid and read at 590 nm using the Biotek synergy H1 microplate reader.

**Flow cytometry and cell sorting:** Cells from culture or directly isolated the previous day from subcutaneous GBM xenografts were used for flow cytometry. Cells were washed with cold DMEM:F12 (Gibco) and counted. Cells were resuspended in 90  $\mu$ L of DMEM:F12 per  $7 \times 10^6$  cells and incubated with GLUT1 (BDBiosciences) or GLUT3 antibody (Invitrogen or R&D), corresponding IgG control, or viability dye for 30 minutes or 15 minutes, respectively. Cells were sorted with the assistance of the Flow Cytometry Core at the University of Alabama at Birmingham. The top and bottom 2–8% was collected for high versus low expression and used for experiments.

**Boyden chamber invasion and migration:**  $5 \times 10^6$  cells were plated on Geltrex (ThermoFisher) and allowed to recover. Media was then replaced low glucose media overnight. 0.8  $\mu$ m pore Boyden chamber inserts coated with reduced growth factor Matrigel (Corning) (Invasion) or non-coated (Migration) were rehydrated for 2 hours prior to plating similar to prior reports [78,79]. 1 mL of DMEM/F12 basal media (Invitrogen) supplemented with epidermal growth factor (EGF), fibroblast growth factor (FGF), sodium pyruvate, penicillin/streptomycin, and the B27 equivalent GEM21 (Gemini Bio Product) was placed in each well of a 24 well plate to be used.  $2.0 \times 10^4$  cells were plated in low glucose media in the Boyden chambers following rehydration in triplicate. Cells were allowed to invade for 8–16 hours or migrate for 4–8 hours depending on cell type, and then fixed with 10% formalin overnight in 4°C. Cells were stained with crystal violet, and then the inserts were washed, cleaned with diH<sub>2</sub>O, and imaged. Six images covering each insert were totaled by hand counting and/or ImageJ particle analysis and graphed using GraphPad Prism. All experiments were performed in duplicate with at least two technical replicates.

**Glycolytic Stress Test:** A Seahorse XFe96 Analyzer (Agilent, Santa Clara, CA) was used to perform a Glycolysis Stress Test (GST) in D456 cells as prior described [80,81]. In Brief, D456 cells were seeded (20,000/well) into a XFe96 cell culture microplate in complete BTIC medium and maintained in a 5% CO<sub>2</sub> incubator at 37°C overnight prior to the experiments. The day of the assay, media in the plate with cells was then changed to assay media (Seahorse basic DMEM

with 2 mM L-glutamine, 1 mM pyruvate at pH 7.4 and 37°C) and maintained in a non-CO<sub>2</sub> incubator at 37 °C for 1 h prior to the assay. The GST was conducted by subsequent injections of glucose (10 mM final concentration), oligomycin (1 µg/mL final concentration), and 2-deoxyglucose (2-DG; 50 mM final concentration). Experiments were performed in triplicate with six technical replicates.

**RNA sequencing analysis:**  $3 \times 10^6$  cells were plated on Geltrex and allowed to recover overnight. Cells were pelleted following overnight incubation with low glucose media and frozen at -80°C until RNA extraction ( $n = 3$  per cell type). RNA extraction was performed using the Norgen Total RNA extraction kit; (Norgen cat. # 37,500, 25,720). RNA quality numbers, RIN, were measured using BioAnalyzer (Agilent) and ranged from (9.7–10 RIN). We used 1000 ng of total RNA as input to the NEBNext Poly(A) mRNA Magnetic Isolation Module (NEB cat# E7490S). PolyA depleted RNA was used as input to the NEBNext Ultra RNA Library Prep Kit for Illumina (NEB cat# E7530S). Libraries were barcoded using the NEBNext Multiplex Oligos for Illumina (NEB cat# E7335S). We pooled all samples to achieve equal representation and sequenced on one lane of an Illumina HiSeq 2500, paired end with 50 base pairs and sequenced an average of 30.78 million reads per sample with an average mean quality score (PF) of 35.23. We processed the raw files using aRNA-pipe which implements STAR for alignment and HTSeq for the generation of count tables [82]. This approach is similar to that previously described in Boyd *et al.* [83]. The differential gene expression (DGE) and GO term enrichment analyses were analyzed in R (version 3.6.2) with RStudio (version 1.2.5033). The raw counts were variance stabilized with DESeq2's (version 1.26.0) varianceStabilizingTransformation function [84]. These variance stabilized counts were used by the prcomp() function for Principal Component Analysis (PCA) analysis. The PCA scatterplot of PC1 and PC2 showed a batch effect (Supplemental Figure 5). The DESeq2 design formula for analyzing differentially expressed genes between GLUT1 and GLUT3 included the experimental groups and this batch effect. Other DESeq2 parameters were at default values. Genes with raw counts average lower than or equal to 10 were excluded in the DESeq2 analysis. Based on the DESeq2 results, genes with an adjusted p-value less than 0.05 and an absolute log<sub>2</sub> fold change greater than 1.0 were considered significant. We converted Ensembl IDs to gene symbols with the R packages ENSDB.Hsapiens.v75 (version 2.99.0) and AnnotationDBI (version 1.48.0) [85,86]. Gene symbols with adjusted p-values and log<sub>2</sub> fold change values from

DESeq2 were used as input for the pathfindR R package (version 1.4.2) [87] to assess gene enrichment by Gene Ontology (GO) terms. We used default parameters for the run\_pathfindR function with the exception of the gene\_sets parameter which was set to 'GO-ALL'. This analysis produced an enrichment chart of the top enriched GO terms and a table of all enriched GO terms. The RNA sequencing data are deposited in GEO: GSE148739.

**Data Set analysis:** SLC2A3 gene expression and tumor site data were downloaded from Oncomine [37,38] for Bittner Ovarian, Tsuji Colon and Cromer Head and Neck cancer datasets to assess expression in primary versus metastatic lesions. SLC2A3 expression data were downloaded from the IVYGAP [35] data to assess the expression of SLC2A3 in various histological regions. TCGA-GBM SPP1 and SLC2A3 gene expression data were downloaded from gliovis [88] and plotted to assess expression correlation. VASARI (Visually AceSable Rembrandt Images) data were downloaded from The Cancer Imaging Archive (TCIA). Data consisted of scores from three radiologists on the full VASARI feature set, including deep white matter invasion (feature number f21). Data from 18 glioblastoma patients that also had REMBRANDT mRNA expression data (Affymetrix GeneChips) were analyzed for GLUT3 expression (probe 202499\_s\_at), GLUT1 expression (probe 201249\_at) and the presence of deep white matter invasion as determined by at least one of the three VASARI radiologists.

### Additional statistical analysis

All statistics not described as executed in R, were performed with GraphPad Prism Version 7 (GraphPad Software Inc., La Jolla, CA). One-way ANOVA and t-tests were performed with Dunnett's or Tukey's test for multiple comparisons with a confidence level of 95%. Correlation analysis was performed using Pearson's correlation analysis with a confidence interval of 95%.

### Acknowledgments

This work was supported by National Institutes of Health grant R21NS096531 to A.B.H. and C.A.-S., 1R01NS104339 to A.B.H, T32NS048039 and F31NS10545801A1 to C.J.L, and startup funds from the University of Alabama at Birmingham for ABH including contributions from the Department of Cell, Developmental and Integrative Biology and the O'Neal Comprehensive Cancer Center. B.N.L. was supported by startup funds from the University of Alabama at Birmingham including contributions from the Department of Cell, Developmental and Integrative Biology, the O'Neal Comprehensive Cancer Center, the Hugh Kaul Precision Medicine Institute, the Center for Clinical and

Translational Science, and the UAB IMPACT fund. J.L.F. was supported by the AMC21 Dean's Research Scholarship. S.J. C. and E.R.G. are supported by funds from the State of Alabama for Cancer Research. A.N.T. is supported by the American Brain Tumor Association Basic Research Fellowship in Honor of Ned Smith and Team Smith Strong (BRF1900021).

## Disclosure statement

The authors declare no conflicts of interest exist.










## Funding

This work was supported by the National Institute of Neurological Disorders and Stroke [R21NS096531]; National Institute of Neurological Disorders and Stroke [1R01NS104339]; National Institute of Neurological Disorders and Stroke [T32NS048039]; National Institute of Neurological Disorders and Stroke [F31NS10545801A1]; American Brain Tumor Association [BRF1900021]; State of Alabama for Cancer Research; University of Alabama at Birmingham.

## Author contributions

C.J.L. designed, performed and analyzed the majority of the studies, and wrote the first draft of the main text. S.G. performed flow sorting experiments. G.A.B performed metabolic flux experiments with analysis assisted by V.D-U. J.L.F., E.R.G., S.J.C., and B.N.L. performed and analyzed RNAseq transcriptomics data. S.Z. and C.A-S. performed computer modeling to illustrate GLUT1/3 structure in the membrane and assisted with writing the manuscript. J.G., A.L., A.B.J, K. T., S.E.W., W.F, and A.N.T. assisted in data collection and analysis. A.B.H is the senior and corresponding author on this manuscript and conceived of the study, provided reagents, designed experiments, wrote and reviewed the manuscript, and approved the final version of the manuscript.

## ORCID

Catherine J Libby  <http://orcid.org/0000-0002-1956-5496>  
 Sajina Gc  <http://orcid.org/0000-0003-2676-2794>  
 Sixue Zhang  <http://orcid.org/0000-0002-2981-9154>  
 Anh Nhat Tran  <http://orcid.org/0000-0003-4292-6760>  
 Emily R. Gordon  <http://orcid.org/0000-0002-0838-7110>  
 Amber B. Jones  <http://orcid.org/0000-0001-8808-4568>  
 Kaysaw Tuy  <http://orcid.org/0000-0003-4197-0129>  
 Sara J. Cooper  <http://orcid.org/0000-0002-9627-0309>  
 Anita B. Hjelmeland  <http://orcid.org/0000-0003-2200-3248>

## References

- [1] Pavlova NN, Thompson CB. The emerging hallmarks of cancer metabolism. *Cell Metab.* 2016;23(1):27–47.
- [2] Libby CJ, McConathy J, Darley-Usmar V, et al. The role of metabolic plasticity in blood and brain stem cell pathophysiology. *Cancer Res.* 2020;80(1):5–16.
- [3] Han T, Kang D, Ji D, et al. How does cancer cell metabolism affect tumor migration and invasion? *Cell Adh Migr.* 2013;7(5):395–403.
- [4] Nakada M, Nakada S, Demuth T, et al. Molecular targets of glioma invasion. *Cell Mol Life Sci.* 2007;64(4):458–478.
- [5] Paw I, Carpenter RC, Watabe K, et al. Mechanisms regulating glioma invasion. *Cancer Lett.* 2015;362(1):1–7.
- [6] Libby CJ, Tran AN, Scott SE, et al. The pro-tumorigenic effects of metabolic alterations in glioblastoma including brain tumor initiating cells. *Biochim Biophys Acta.* 2018;1869(2):175–188.
- [7] Hottinger AF, Stupp R, Homicsko K. Standards of care and novel approaches in the management of glioblastoma multiforme. *Chin J Cancer.* 2014;33(1):32–39.
- [8] Bogdahn U. Chemosensitivity of malignant human brain tumors. Preliminary results. *J Neurooncol.* 1983;1(2):149–166.
- [9] Simpson JR, et al. Influence of location and extent of surgical resection on survival of patients with glioblastoma multiforme: results of three consecutive Radiation Therapy Oncology Group (RTOG) clinical trials. *Int J Radiat Oncol Biol Phys.* 1993;26(2):239–244.
- [10] Reardon DA, Rich JN, Friedman HS, et al. Recent advances in the treatment of malignant astrocytoma. *J Clin Oncol.* 2006;24(8):1253–1265.
- [11] Stummer W, Reulen H-J, Meinel T, et al. Extent of resection and survival in glioblastoma multiforme: identification of and adjustment for bias. *Neurosurgery.* 2008;62(3):564–576.
- [12] Stummer W, Beck T, Beyer W, et al. Long-sustaining response in a patient with non-resectable, distant recurrence of glioblastoma multiforme treated by interstitial photodynamic therapy using 5-ALA: case report. *J Neurooncol.* 2008;87(1):103–109.
- [13] Labak CM, Wang PY, Arora R, et al. Glucose transport: meeting the metabolic demands of cancer, and applications in glioblastoma treatment. *Am J Cancer Res.* 2016;6(8):1599–1608.
- [14] Barron CC, Bilan PJ, Tsakiridis T, et al. Facilitative glucose transporters: implications for cancer detection, prognosis and treatment. *Metabolism.* 2016;65(2):124–139.
- [15] Simpson IA, Dwyer D, Malide D, et al. The facilitative glucose transporter GLUT3: 20 years of distinction. *Am J Physiol Endocrinol Metab.* 2008;295(2):E242–E253.
- [16] Macheda ML, Rogers S, Best JD. Molecular and cellular regulation of glucose transporter (GLUT) proteins in cancer. *J Cell Physiol.* 2005;202(3):654–662.
- [17] Vannucci RC, Vannucci SJ. Glucose metabolism in the developing brain. *Semin Perinatol.* 2000;24(2):107–115.
- [18] Vannucci SJ, Clark RR, Koehler-Stec E, et al. Glucose transporter expression in brain: relationship to cerebral glucose utilization. *Dev Neurosci.* 1998;20(4-5):369–379.
- [19] Boado RJ, Black KL, Pardridge WM. Gene expression of GLUT3 and GLUT1 glucose transporters in human

- brain tumors. *Brain Res Mol Brain Res.* 1994;27(1):51–57.
- [20] Benarroch EE. Brain glucose transporters: implications for neurologic disease. *Neurology.* 2014;82(15):1374–1379.
- [21] Flavahan WA, Wu Q, Hitomi M, et al. Brain tumor initiating cells adapt to restricted nutrition through preferential glucose uptake. *Nat Neurosci.* 2013;16(10):1373–1382.
- [22] Ruiz-Ontanon P, Orgaz JL, Aldaz B, et al. Cellular plasticity confers migratory and invasive advantages to a population of glioblastoma-initiating cells that infiltrate peritumoral tissue. *Stem Cells.* 2013;31(6):1075–1085.
- [23] Ortensi B, Setti M, Osti D, et al. Cancer stem cell contribution to glioblastoma invasiveness. *Stem Cell Res Ther.* 2013;4(1):18.
- [24] Kuang R, Jahangiri A, Mascharak S, et al. GLUT3 upregulation promotes metabolic reprogramming associated with antiangiogenic therapy resistance. *JCI Insight.* 2017;2(2):e88815. DOI:10.1172/jci.insight.88815.
- [25] Keunen O, Johansson M, Oudin A, et al. Anti-VEGF treatment reduces blood supply and increases tumor cell invasion in glioblastoma. *Proc Natl Acad Sci U S A.* 2011;108(9):3749–3754.
- [26] Osawa T, Shibuya M. Targeting cancer cells resistant to hypoxia and nutrient starvation to improve anti-angiogenic therapy. *Cell Cycle.* 2013;12(16):2519–2520.
- [27] Ye F, Zhang Y, Liu Y, et al. Protective properties of radio-chemoresistant glioblastoma stem cell clones are associated with metabolic adaptation to reduced glucose dependence. *PLoS One.* 2013;8(11):e80397.
- [28] Fack F, Espedal H, Keunen O, et al. Bevacizumab treatment induces metabolic adaptation toward anaerobic metabolism in glioblastomas. *Acta Neuropathol.* 2015;129(1):115–131.
- [29] Boral D, Vishnoi M, Liu HN, et al. Molecular characterization of breast cancer CTCs associated with brain metastasis. *Nat Commun.* 2017;8(1):196. DOI:10.1038/s41467-017-00196-1.
- [30] Kuo MH, Chang W-W, Yeh B-W, et al. Glucose Transporter 3 is essential for the survival of breast cancer cells in the brain. *Cells.* 2019;8(12):1568.
- [31] Gao H, Hao Y, Zhou X, et al. Prognostic value of glucose transporter 3 expression in hepatocellular carcinoma. *Oncol Lett.* 2020;19(691–699).
- [32] Masin M, Vazquez J, Rossi S, et al. GLUT3 is induced during epithelial-mesenchymal transition and promotes tumor cell proliferation in non-small cell lung cancer. *Cancer Metab.* 2014;2:11. doi:10.1186/2049-3002-2-11.
- [33] Kuo CC, Ling -H-H, Chiang M-C, et al. Metastatic colorectal cancer rewrites metabolic program through a Glut3-YAP-dependent signaling circuit. *Theranostics.* 2019;9(9):2526–2540.
- [34] Cosset É, Ilmjärv S, Dutoit V, et al. Glut3 addiction is a druggable vulnerability for a molecularly defined subpopulation of glioblastoma. *Cancer Cell.* 2017;32(6):856–868.e855.
- [35] Puchalski RB, Shah N, Miller J, et al. An anatomic transcriptional atlas of human glioblastoma. *Science.* 2018;360(6389):660–663.
- [36] Flavahan WA, Case Western Reserve University School of Graduate Studies, (2013).
- [37] Rhodes DR, Kalyana-Sundaram S, Mahavisno V, et al. OncoPrint 3.0: genes, pathways, and networks in a collection of 18,000 cancer gene expression profiles. *Neoplasia.* 2007;9(2):166–180.
- [38] Rhodes DR, Yu J, Shanker K, et al. ONCOMINE: a cancer microarray database and integrated data-mining platform. *Neoplasia.* 2004;6(1):1–6.
- [39] Madhavan S, Zenklusen J-C, Kotliarov Y, et al. Rembrandt: helping personalized medicine become a reality through integrative translational research. *Mol Cancer Res.* 2009;7(2):157–167.
- [40] Inukai K, Shewan AM, Pascoe WS, et al. Carboxy terminus of glucose transporter 3 contains an apical membrane targeting domain. *Mol Endocrinol.* 2004;18(2):339–349.
- [41] Pietras A, Katz A, Ekström E, et al. Osteopontin-CD44 signaling in the glioma perivascular niche enhances cancer stem cell phenotypes and promotes aggressive tumor growth. *Cell Stem Cell.* 2014;14(3):357–369.
- [42] Chandran UR, Ma C, Dhir R, et al. Gene expression profiles of prostate cancer reveal involvement of multiple molecular pathways in the metastatic process. *BMC Cancer.* 2007;7:1. DOI:10.1186/1471-2407-7-64.
- [43] McClung HM, Golembieski WA, Schultz CR, et al. Deletion of the SPARC acidic domain or EGF-like module reduces SPARC-induced migration and signaling through p38 MAPK/HSP27 in glioma. *Carcinogenesis.* 2012;33(2):275–284.
- [44] Alam R, Schultz CR, Golembieski WA, et al. PTEN suppresses SPARC-induced pMAPKAPK2 and inhibits SPARC-induced Ser78 HSP27 phosphorylation in glioma. *Neuro Oncol.* 2013;15(4):451–461.
- [45] Schiemann BJ, Neil JR, Schiemann WP. SPARC inhibits epithelial cell proliferation in part through stimulation of the transforming growth factor-beta-signaling system. *Mol Biol Cell.* 2003;14(10):3977–3988.
- [46] McClung HM, Thomas SL, Osenkowski P, et al. SPARC upregulates MT1-MMP expression, MMP-2 activation, and the secretion and cleavage of galectin-3 in U87MG glioma cells. *Neurosci Lett.* 2007;419(2):172–177.
- [47] Shi Q, Bao S, Song L, et al. Targeting SPARC expression decreases glioma cellular survival and invasion associated with reduced activities of FAK and ILK kinases. *Oncogene.* 2007;26(28):4084–4094.
- [48] Shirakihara T, Kawasaki T, Fukagawa A, et al. Identification of integrin  $\alpha 3$  as a molecular marker of cells undergoing epithelial-mesenchymal transition and of cancer cells with aggressive phenotypes. *Cancer Sci.* 2013;104(9):1189–1197.
- [49] Mueckler M, Thorens B. The SLC2 (GLUT) family of membrane transporters. *Mol Aspects Med.* 2013;34(2–3):121–138.
- [50] Bunn RC, Jensen MA, Reed BC. Protein interactions with the glucose transporter binding protein GLUT1CBP that provide a link between GLUT1

- and the cytoskeleton. *Mol Biol Cell*. 1999;10(4):819–832.
- [51] Xia S, Lal B, Tung B, et al. Tumor microenvironment tenascin-C promotes glioblastoma invasion and negatively regulates tumor proliferation. *Neuro Oncol*. 2016;18(4):507–517.
- [52] Wei Z, Ma W, Qi X, et al. Pinin facilitated proliferation and metastasis of colorectal cancer through activating EGFR/ERK signaling pathway. *Oncotarget*. 2016;7(20):29429–29439.
- [53] Knapp B, Wolfrum U. Adhesion GPCR-related protein networks. *Handb Exp Pharmacol*. 2016;234:147–178.
- [54] Neagu MR, Gill CM, Batchelor TT, et al. Genomic profiling of brain metastases: current knowledge and new frontiers. *Chin Clin Oncol*. 2015;4(2):22.
- [55] Lagal V, Abrivard M, Gonzalez V, et al. Spire-1 contributes to the invadosome and its associated invasive properties. *J Cell Sci*. 2014;127(Pt 2):328–340.
- [56] Wen Q, Li N, Xiao X, et al. Actin nucleator Spire 1 is a regulator of ectoplasmic specialization in the testis. *Cell Death Dis*. 2018;9(2):208. DOI:10.1038/s41419-017-0201-6.
- [57] Zhao C, Shen Y, Tao X, et al. Silencing of CtBP1 suppresses the migration in human glioma cells. *J Mol Histol*. 2016;47(3):297–304.
- [58] Korgun ET, Celik-Ozenci C, Seval Y, et al. Do glucose transporters have other roles in addition to placental glucose transport during early pregnancy? *Histochem Cell Biol*. 2005;123(6):621–629.
- [59] Lu S, Wang Y. Nonmetabolic functions of metabolic enzymes in cancer development. *Cancer Commun (Lond)*. 2018;38(1):63.
- [60] Huangyang P, Simon MC. Hidden features: exploring the non-canonical functions of metabolic enzymes. *Dis Model Mech*. 2018;11(8):dmm033365.
- [61] Boukouris AE, Zervopoulos SD, Michelakis ED. Metabolic enzymes moonlighting in the nucleus: metabolic regulation of gene transcription. *Trends Biochem Sci*. 2016;41(8):712–730.
- [62] Jan HJ, Lee -C-C, Shih Y-L, et al. Osteopontin regulates human glioma cell invasiveness and tumor growth in mice. *Neuro Oncol*. 2010;12(1):58–70.
- [63] Shevde LA, Samant RS. Role of osteopontin in the pathophysiology of cancer. *Matrix Biol*. 2014;37:131–141.
- [64] Park JB, Kwak HJ, Lee SH. Role of hyaluronan in glioma invasion. *Cell Adh Migr*. 2008;2(3):202–207.
- [65] Morath I, Hartmann TN, Orian-Rousseau V. CD44: more than a mere stem cell marker. *Int J Biochem Cell Biol*. 2016;81(Pt A):166–173.
- [66] Olmez I, Shen W, McDonald H, et al. Dedifferentiation of patient-derived glioblastoma multiforme cell lines results in a cancer stem cell-like state with mitogen-independent growth. *J Cell Mol Med*. 2015;19(6):1262–1272.
- [67] Soeda A, Park M, Lee D, et al. Hypoxia promotes expansion of the CD133-positive glioma stem cells through activation of HIF-1alpha. *Oncogene*. 2009;28(45):3949–3959.
- [68] Liu G, Yuan X, Zeng Z, et al. Analysis of gene expression and chemoresistance of CD133+ cancer stem cells in glioblastoma. *Mol Cancer*. 2006;5:67.
- [69] Orian-Rousseau V. CD44 acts as a signaling platform controlling tumor progression and metastasis. *Front Immunol*. 2015;6:154.
- [70] Cuddapah VA, Robel S, Watkins S, et al. A neurocentric perspective on glioma invasion. *Nat Rev Neurosci*. 2014;15(7):455–465.
- [71] Ansardamavandi A, Tafazzoli-Shadpour M, Shokrgozar MA. Behavioral remodeling of normal and cancerous epithelial cell lines with differing invasion potential induced by substrate elastic modulus. *Cell Adh Migr*. 2018;12(5):472–488.
- [72] Walker K, Hjelmeland A. Method for efficient transduction of cancer stem cells. *J Cancer Stem Cell Res*. 2014;2.
- [73] Omasits U, Ahrens CH, Müller S, et al. Protter: interactive protein feature visualization and integration with experimental proteomic data. *Bioinformatics*. 2014;30(6):884–886.
- [74] Boyd NH, Walker K, Fried J, et al. Addition of carbonic anhydrase 9 inhibitor SLC-0111 to temozolomide treatment delays glioblastoma growth in vivo. *JCI Insight*. 2017;2(24). DOI:10.1172/jci.insight.92928.
- [75] Tran AN, Boyd NH, Walker K, et al. NOS expression and NO function in glioma and implications for patient therapies. *Antioxid Redox Signal*. 2017;26(17):986–999.
- [76] Yang F, Li B, Yang Y, et al. Leptin enhances glycolysis via OPA1-mediated mitochondrial fusion to promote mesenchymal stem cell survival. *Int J Mol Med*. 2019;44(1):301–312.
- [77] Jones RB, Dorsett KA, Hjelmeland AB, et al. The ST6Gal-I sialyltransferase protects tumor cells against hypoxia by enhancing HIF-1α signaling. *J Biol Chem*. 2018;293(15):5659–5667.
- [78] Justus CR, Leffler N, Ruiz-Echevarria M, et al. 2014. In vitro cell migration and invasion assays. *J Vis Exp*. 2014;88. DOI: 10.3791/51046.
- [79] Wang SD, Rath P, Lal B, et al. EphB2 receptor controls proliferation/migration dichotomy of glioblastoma by interacting with focal adhesion kinase. *Oncogene*. 2012;31(50):5132–5143.
- [80] Libby CJ, Zhang S, Benavides GA, et al. Identification of compounds that decrease glioblastoma growth and glucose uptake in vitro. *ACS Chem Biol*. 2018;13(8):2048–2057.
- [81] Rai G, Brimacombe KR, Mott BT, et al. Discovery and optimization of potent, cell-active pyrazole-based inhibitors of lactate dehydrogenase (LDH). *J Med Chem*. 2017;60(22):9184–9204.
- [82] Alonso A, Lasseigne BN, Williams K, et al. aRNAPipe: a balanced, efficient and distributed pipeline for processing RNA-seq data in high-performance computing environments. *Bioinformatics*. 2017;33(11):1727–1729.
- [83] Boyd NH, Walker K, Ayokanmbi A, et al. Chromodomain Helicase DNA-Binding Protein 7 is suppressed in the perinecrotic/ischemic microenvironment and is a novel regulator of glioblastoma angiogenesis. *Stem Cells*. 2019;37(4):453–462.
- [84] Love MI, Huber W, Anders S. Moderated estimation of fold change and dispersion for RNA-seq data with

- DESeq2. *Genome Biol.* **2014**;15(12):550. DOI:[10.1186/s13059-014-0550-8](https://doi.org/10.1186/s13059-014-0550-8).
- [85] Rainer J. *EnsDb.Hsapiens.v75*: Ensembl based annotation package. (R package version 2.99.0., **2017**).
- [86] Pagès H, Carlson M, Falcon S, et al. *AnnotationDbi*: Manipulation of SQLite-based annotations in Bioconductor. (R package version 1.48.0., **2019**).
- [87] Ulgen E, Ozisik O, Sezerman OU. *pathfindR*: an R package for comprehensive identification of enriched pathways in omics data through active subnetworks. *Front Genet.* **2019**;10:858.
- [88] Bowman RL, Wang Q, Carro A, et al. *GlioVis* data portal for visualization and analysis of brain tumor expression datasets. *Neuro Oncol.* **2017**;19(1):139–141.